Comparison of polarizable and nonpolarizable models of hydrogen fluoride in liquid and supercritical states: A Monte Carlo simulation study

Pál Jedlovszky[a)]
Department of Physiology and Biophysics, Mount Sinai School of Medicine, New York, New York 10029, and Istituto Nazionale per la Fisica della Materia e Dipartimento di Fisica, Università degli Studi di Trento, I-38050 Povo (Trento), Italy

Mihaly Mezei
Department of Physiology and Biophysics, Mount Sinai School of Medicine, New York, New York 10029

Renzo Vallauri
Istituto Nazionale per la Fisica della Materia e Dipartimento di Fisica, Università degli Studi di Trento, I-38050 Povo (Trento), Italy

(Received 13 June 2001; accepted 6 September 2001)

Structural and thermodynamic properties of a polarizable and two pairwise additive effective interaction potential models of hydrogen fluoride are analyzed and compared with experimental data in the liquid and supercritical phase as well as along the vapor–liquid coexistence line. Pair correlation functions and thermodynamic data are obtained from Monte Carlo simulations at two liquid and four supercritical thermodynamic state points. Vapor–liquid equilibrium properties have been calculated from a set of Gibbs ensemble Monte Carlo simulations. It is found that the polarizable model is clearly superior over the two nonpolarizable ones in describing the temperature and density variation of several thermodynamic and structural properties. Thus the experimentally observed elongation of the hydrogen bonds with decreasing density is only reproduced by the polarizable model. Similarly, among the three models only the polarizable one can correctly describe the dependence of the density on the pressure and temperature in the entire range of the liquid state, although the density of this model is always somewhat lower than that of real HF. Consistently, the vapor–liquid coexistence curve is also much better reproduced by the polarizable than by the other two models. All three models underestimate the critical temperature, although the polarizable model is again in a considerably better agreement with the experimental data than the other two. All three models reproduce the experimental fact that the energy of evaporation of HF goes through a maximum as a function of the temperature. © *2001 American Institute of Physics.*
[DOI: 10.1063/1.1413973]

I. INTRODUCTION

The investigation of the structural and dynamical properties of various hydrogen-bonded liquids (e.g., water,[1–15] methanol,[13,16–19] ethanol,[20,21] formic acid,[22–25] ammonia,[26,27] etc.) by computer simulation methods has received considerable attention in the past decade. However, despite the fact that liquid hydrogen fluoride is one of the most strongly associating liquids, interest has only turned toward this liquid in the past few years. One of the reasons of this is the fact that, due to its extremely high reactivity, very little experimental information is available for liquid HF. The limited amount of available experimental data has prevented a detailed comparison of the performance of various potential models so far. The results of the first diffraction experiment performed on liquid hydrogen fluoride[28] made clear that only those potential models, which account not only for the dipole but also for the quadrupole moment of the HF molecules, can reliably describe the molecular level structure of the liquid. Such models usually consist of three charged interaction sites: the H and F atoms carry fractional positive charges, and a fractional negative charge is located at an additional site along the H–F bond.[29–33] On the other hand, two-site models[29,34–36] are not able to reproduce the experimental pair correlation function of liquid HF, even in a qualitative way.[28] The reason for this is that in liquid HF the molecules are arranged in long hydrogen-bonded chains, in which the neighbors are preferentially forming tetrahedral angle around the hydrogen acceptor F atom.[37,38] This tilt of the chains around the F atom is an effect of the quadrupole moment of the molecules, and hence it cannot be reproduced by two-site models.

Many of the HF potential models have been parameterized by fitting results of *ab initio* calculations of clusters built up by a few HF molecules.[29,33–36] Such models can, in general, well describe the properties of HF vapor,[33,39,40] and, in some cases, also of crystalline HF.[33] However, due to the unusually large cooperativity of the molecules, these models fail to reproduce the thermodynamic properties of the liquid phase.[31,33] For instance, at 20 °C the internal energy of the three-site model of Klein and McDonald[29] and that of Della

[a)]Author to whom correspondence should be addressed. Present address: Department of Colloid Chemistry, Eotvos Lorand University, H-1117 Budapest, Pázmány Péter stny 1/a, Hungary. Electronic mail: pali@cric.chemres.hu

Valle and Gazzillo[33] is about 30% and 50% larger (i.e., less attractive) than the experimental value.[30,33] Conversely, effective pair potential models, which have been parameterized to reproduce various properties of liquid HF, such as the TIPS model of Cournoyer and Jorgensen[30] and a model recently developed by two of us (referred here as JV-NP),[31] cannot account for the properties of the isolated dimer.[30,32] On the other hand, these two models have been proved to be the most successful pairwise additive potentials in describing the properties of liquid HF so far. The JV-NP model has successfully been used in recent studies of both single molecule[41,42] and collective[43,44] dynamics of liquid HF. It has also been shown by Visco and Kofke that the TIPS model describes the properties of the liquid–vapor equilibrium of hydrogen fluoride considerably better than pair potentials developed by fitting dimer properties.[45,46] In a recent study Martín *et al.* demonstrated that the liquid–vapor coexistence curve can be reproduced by the JV-NP model about as well as by TIPS.[47]

Besides this drawback of the pairwise additive potential models of not being able to reproduce the properties of both liquid HF and the isolated HF dimer at the same time, it has also been shown by Fries and Richardi that both *ab initio* based and effective pair potential models strongly underestimate the dielectric constant.[48] They have argued that this is due to the fact that these models do not account for the polarization of the molecules. In order to overcome these problems we have proposed a polarizable potential model of hydrogen fluoride.[32] This model, referred here as JV-P, explicitly takes into account three-particle interactions as it lets the dipole moment of the molecules change according to the electric field of the surrounding molecules. In this way, this model can, at least partly, account for the large cooperativity of the molecules. Indeed, it has been found that the JV-P model can reasonably well describe the properties of both the isolated HF dimer and the liquid phase of HF.[32] In particular, unlike pairwise additive potentials, this model can reproduce the experimentally observed elongation of the F$\cdots$F separation of hydrogen-bonded neighbors when moving from the liquid to the gas phase.[32] It should be noted that similar effect has been observed in water: polarizable water models, in accordance with the experimental data, are found to induce an elongation of the hydrogen bonds when moving from ambient to supercritical conditions, whereas nonpolarizable models did not show such an elongation.[7,10,11] It has also been found that the polarizable JV-P model can reproduce the density of HF well in the entire temperature range of its liquid state at atmospheric pressure.[32] This is again in contrast with the behavior of the nonpolarizable TIPS and JV-NP models, the density of which have been found to increase too strongly with decreasing temperature.[31,32]

Recently Pfleiderer *et al.* reported results of neutron scattering experiments on deuterated hydrogen fluoride.[49] The thermodynamic states covered by these experiments range from ambient to supercritical conditions. This new experimental information now allows a detailed comparison of the properties of different HF models in a very broad range of thermodynamic conditions, including both liquid and supercritical states. The effect of the density (or pressure) of the system along a supercritical isotherm as well as that of the temperature along an isochore can also be investigated.

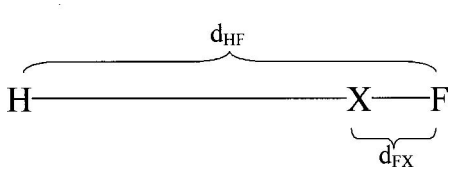

FIG. 1. Schematic representation of the geometry of the HF models investigated.

In this paper such a comparison is made for the nonpolarizable TIPS, JV-NP, and for the polarizable JV-P models. Pair correlation functions and thermodynamic properties of the models are calculated at several liquid and supercritical state points. Vapor–liquid equilibrium properties of the models are also determined. The paper is organized as follows. In Secs. II and III details of the potential models tested and the simulations performed, respectively, are given. In Sec. IV structural, whereas in Sec. V thermodynamic properties of the models are discussed. In Sec. VI results of the vapor–liquid equilibrium of the models are given. Finally, in Sec. VII, some conclusions are drawn.

II. POTENTIAL MODELS

The three potential models tested are all based on the same principles. All of them belong to the group of the effective potential models, parameterized to reproduce properties of liquid HF at atmospheric pressure and room temperature. The models describe the HF molecule by three linearly arranged interaction sites. The H and F atoms, separated by the distance d_{HF}, carry fractional positive charges of $+q$. The third site, denoted by X, is located along the H–F bond at a distance of d_{FX} from the F atom. This site carries a fractional negative charge of $-2q$. The non-Coulombic part of the potential is described by a Lennard-Jones interaction, acting between the F atoms. In the case of the JV-P model the polarization of the molecules due to the local electric field of their environment is also taken explicitly into account. Thus at the position of the F atom of the ith molecule a point dipole of $\underline{\mu}_i^{\mathrm{ind}}$ is induced by the local electric field $\underline{E}_i$ according to the equation

$$\underline{\mu}_i^{\mathrm{ind}} = \alpha \underline{E}_i = \alpha(\underline{E}_i^q + \underline{E}_i^\mu), \tag{1}$$

where $\underline{E}_i^q$ and $\underline{E}_i^\mu$ are the electric field contributions due to the permanent charges and induced dipole moments of the other molecules, and α is the (scalar) polarizability of the molecule. A schematic representation of the geometry of the models is shown in Fig. 1, whereas their geometry and interaction parameters as well as the permanent dipole and quadrupole moments (m and θ_{zz}, respectively) are summarized in Table I.

In calculating the energy of the system all interactions between molecules separated by a F–F distance r_{FF} larger than the cutoff value of $R_C = 9.0$ Å has been truncated to zero. The electrostatic contribution of the distant molecular

TABLE I. Parameters describing the potential models tested.

	d_{HF}/Å	d_{FX}/Å	q/e	σ/Å	$(\varepsilon/k_B)/K$	α/Å^3	m/D	θ_{zz}/B
TIPS	0.917	0.166	0.725	3.00	75.8	-	2.04	2.55
JV-NP	0.973	0.1647	0.592	2.83	60.0	-	1.83	2.36
JV-P	0.973	0.1647	0.592	3.05	110.0	0.83	1.83	2.36

pairs to the total energy has been taken into account by the reaction field correction method,[50–52] whereas their Lennard-Jones contribution has been estimated by the assumption that the $g_{FF}(r)$ partial pair correlation function is equal to unity beyond R_C.[53] Thus the total energy of the simulated system has been calculated by the equation

$$U=\sum_{i=1}^{N}\sum_{j=i+1}^{N} u_{ij}+U^{\mathrm{POL}}+U^{\mathrm{corr}}, \tag{2}$$

where u_{ij} is the pair interaction energy between the ith and jth molecule (including the reaction field correction term for the charge–charge interactions[51]):

$$u_{ij}=\begin{cases} 4\varepsilon\left[\left(\dfrac{\sigma}{r_{\mathrm{FF}}}\right)^{12}-\left(\dfrac{\sigma}{r_{\mathrm{FF}}}\right)^{6}\right]+\dfrac{1}{4\pi\in_0}\left[\dfrac{c_{RF}}{2}Nm_i^2+\displaystyle\sum_{A=1}^{3}\sum_{B=1}^{3}\frac{q_Aq_B}{r_{iA,jB}}\left(1+\frac{c_{RF}}{2}(r_{iA,jB})^3\right)\right] & \text{if } r_{\mathrm{FF}}<R_C \\ 0 & \text{if } r_{\mathrm{FF}}\geqslant R_C \end{cases}, \tag{3}$$

and U^{corr} is the long range correction for the Lennard-Jones interactions:

$$U^{\mathrm{corr}}=\frac{8\pi}{9}\frac{N\rho_m}{R_C^3}\varepsilon\sigma^6\left[\left(\frac{\sigma}{R_C}\right)^6-3\right]. \tag{4}$$

Here c_{RF} is the reaction field correction factor:

$$c_{RF}=\frac{2(\in_{RF}-1)}{2\in_{RF}+1}R_C^{-3}, \tag{5}$$

$\in_0$ is the vacuum permittivity, $\in_{RF}$ is the dielectric constant of the continuum surrounding the sphere of radius R_C around the central molecule, σ and ε are the Lennard-Jones parameters, ρ_m is the molecular number density of the system, m_i is the permanent dipole moment of the ith molecule, indices A and B run through all the sites of the molecule, q_A and q_B are the fractional charges of sites A and B, respectively, and $r_{iA,jB}$ is the distance of site A on molecule i from site B on molecule j. For the JV-P model, the energy contribution of the polarization of the molecules U^{POL} has been calculated as[32]

$$U^{\mathrm{POL}}=-\frac{1}{2}\sum_{i=1}^{N}\underline{\mu}_i^{\mathrm{ind}}\underline{E}_i^q. \tag{6}$$

As seen from Eq. (1), the calculation of the $\underline{\mu}_i^{\mathrm{ind}}$ induced point dipole vectors requires the knowledge of both $\underline{E}_i^q$ and $\underline{E}_i^{\mu}$. Taking the reaction field correction terms also into account,[52] these vectors can be expressed as

$$\underline{E}_i^q=\frac{1}{4\pi\in_0}\times\left[c_{RF}\underline{m}_i+\sum_{\substack{j=1\\0<r_{\mathrm{FF}}<R_C}}^{N}\sum_{A=1}^{3}\frac{q_A\underline{r}_{i,jA}}{r_{i,jA}^3}(1-c_{RF}r_{i,jA}^3)\right] \tag{7}$$

and

$$\underline{E}_i^{\mu}=\frac{1}{4\pi\in_0}\left[c_{RF}\underline{\mu}_i^{\mathrm{ind}}+\sum_{\substack{j=1\\0<r_{\mathrm{FF}}<R_C}}^{N}\frac{1}{r_{ij}^3}\times\left[\frac{3\underline{r}_{ij}\underline{\mu}_j^{\mathrm{ind}}}{r_{ij}^2}\underline{r}_{ij}-\underline{\mu}_j^{\mathrm{ind}}(1-c_{RF}r_{ij}^3)\right]\right]. \tag{8}$$

In these equations $\underline{r}_{i,jA}$ and $\underline{r}_{ij}$ denote the vectors pointing from site A of molecule j, and from the position of the induced dipole moment (i.e., the F atom) of molecule j, respectively, to the position of the point dipole induced on molecule i. As is evident from Eqs. (1) and (8), the expression of $\underline{\mu}_i^{\mathrm{ind}}$ contains also the dipole moments induced on the other molecules of the system. Therefore, the induced dipole moments can only be determined by solving the set of N vectorial linear equations given by Eq. (1). This set of equation can, in practice, only be solved by using an iterative procedure.

TABLE II. Thermodynamic parameters of the simulated state points.

State point	T/K	ρ_m/Å^{-3}	p/bar
I	300	0.0290	2
II	373	0.0240	12
III	473	0.0240	319
IV	473	0.0195	166
V	473	0.0120	84
VI	473	0.0071	78

III. MONTE CARLO SIMULATIONS

A. Liquid and supercritical state simulations

Monte Carlo simulations have been performed both on the (N,V,T) and (N,p,T) ensemble at the six thermodynamic state points at which the neutron diffraction experiments of Pfleiderer *et al.*[49] have been carried out. The temperature, pressure, and molecular number density values corresponding to these state points are summarized in Table II. State point I represents nearly ambient conditions. State point II is close to the experimental vapor–liquid coexistence curve (at 12 bar liquid HF boils at 376 K). The supercritical state point III corresponds to the same density as the liquid state point II, whereas state points III–VI lay along a supercritical isotherm.

In each simulation 256 HF molecules have been placed into the cubic simulation box. Usual periodic boundary conditions have been applied. At each Monte Carlo step a randomly selected molecule has been translated by a random distance of maximum 0.3 Å, and rotated around a randomly chosen space-fixed axis by no more than 10°. In the (N,p,T) ensemble simulations every 256 of these steps have been followed by a volume change trial, in which the volume of the simulation box has been attempted to change by no more than 400 Å^3. In simulations with the polarizable JV-P model the induced dipole moment of the molecules have been determined from Eq. (1) by iteration after every Monte Carlo step. At the beginning of the entire simulation the μ_i^{ind} values have been set to zero, and in each iteration their initial values have been taken from the previous configuration. The iteration has stopped when the set of the induced dipoles has changed less than 0.1% in one iteration step. Since one single Monte Carlo move resulted only in a very small perturbation of the charge distribution of the system, the iteration has converged rapidly, usually after the first step.

Systems have been equilibrated by 5–10 million Monte Carlo moves. The calculated properties have been averaged over 20 000 equilibrium configurations, separated by 256 particle displacement steps and, in the case of the (N,p,T) ensemble simulations, one volume change step each. The simulations with the polarizable JV-P model required about 3 weeks long runs on a single R10000 processor. Nonpolarizable simulations have been completed within a few days.

B. Simulation of the vapor–liquid equilibrium

The phase diagram of the vapor–liquid equilibrium of the models has been determined by performing a set of Gibbs ensemble Monte Carlo (GEMC) simulations[54] at temperatures separated by 25 K in the interval between 200 K and 425 K. In the simulations the overall density of the system (i.e., the sum of the volume of the two simulation cells as well as the total number of molecules in the two systems) has been kept fixed. Cubic simulation boxes and standard periodic boundary conditions have been used. In the simulations with the nonpolarizable models the two systems have contained 400 molecules altogether. In the simulations using the polarizable JV-P model this number had to be reduced to 256 because of the large computing time required. In every simulation each pair of particle displacement steps (i.e., one step in each box) has been followed by a particle transfer step, in which the transfer of a randomly selected molecule has been attempted from one simulation box to the other. Volume exchange steps have been performed after every 250 pairs of particle displacement steps. In a particle displacement step a randomly selected particle has been translated by no more than 0.3 Å and rotated around a randomly chosen space fixed axis by no more than 15°. In a volume exchange step the volume of one of the boxes has randomly been increased at the expense of the volume of the other box by no more than 200 Å^3. In the low temperature simulations the steps of transferring a molecule from the vapor to the liquid phase have been done by using cavity biased insertion.[55] Thus analogously to the cavity biased grand canonical ensemble Monte Carlo simulation method,[56,57] the transferred molecule has only been attempted to be inserted into cavities having a radius of at least 2.6 Å. Suitable cavities have been searched along a $50\times50\times50$ grid.

The description of the polarization of the molecules by induced point dipoles has a known drawback that in cases when the distance of two molecules becomes shorter than a critical value, the dipole moments of the two molecules tend to be infinitely large.[58,59] This polarization catastrophe has no physical meaning; it is simply a failure of the iterative algorithm. The critical distance below which such polarization catastrophe can occur is well below the closest possible approach of the neighbors allowed by the Lennard-Jones repulsion, and hence this polarization catastrophe can usually be prevented simply by the fact that the molecules cannot approach each other sufficiently closely. However, in a particle transfer step of the GEMC simulation the inserted particle can easily be put close enough to another molecule for such a polarization catastrophe to occur. Therefore, in the simulations with the JV-P model we have rejected particle transfer steps in which the F atom of the inserted molecule became closer to another F atom than 2.0 Å without any further test. This cutoff distance has been chosen in the range where the $g_{\mathrm{FF}}(r)$ partial pair correlation function is still zero (it becomes different from zero only around 2.4 Å for the JV-P model[32]), and hence the use of such a preliminary test of the particle insertion should not affect the results of the simulation. In this way the occurrence of the polarization catastrophe has successfully been avoided.

The systems have been equilibrated by 5–10 million pairs of particle displacement steps. The coexisting liquid and vapor densities have then been determined in the production phase of 4.5 million pairs of particle displacement steps. For further analyses, 10 pairs of configurations, sepa-

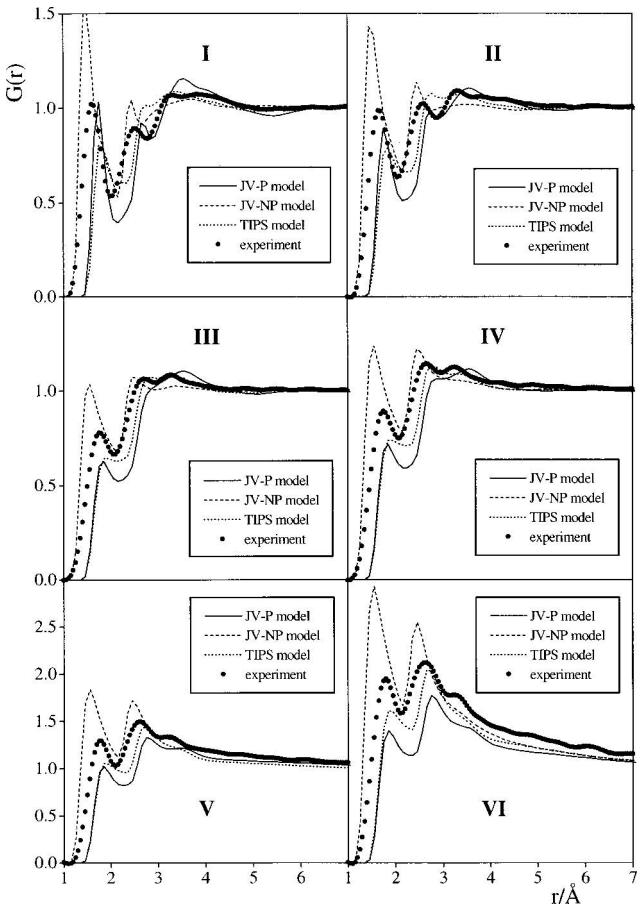

FIG. 2. Comparison of the total pair correlation function $G(r)$ of deuterated HF as obtained from neutron diffraction experiment (Ref. 49) and from (N,V,T) Monte Carlo simulations using the three tested potential models at six different thermodynamic state points.

rated by 0.5 million pairs of particle displacement steps each, have been saved at each temperature.

IV. STRUCTURAL RESULTS

The total pair correlation function $G(r)$ of deuterated HF, obtained from the neutron diffraction experiment of Pfleiderer *et al.*,[49] is compared in Fig. 2 with the corresponding functions of the three models, as resulted from (N,V,T) ensemble simulations at the thermodynamic state points I–VI. In the simulations, $G(r)$ can simply be calculated as the weighed average of the three partial pair correlation functions

$$G(r)=0.210g_{\mathrm{FF}}(r)+0.497g_{\mathrm{FH}}(r)+0.293g_{\mathrm{HH}}(r). \qquad (9)$$

The results at state point I are consistent with the findings of previous comparisons,[31,32] performed at slightly different thermodynamic conditions using a different experimental data set.[28] Thus the first (hydrogen-bonding) peak of the JV-NP model is located at too small r values and it is considerably higher than the experimental peak. Conversely, the TIPS model overestimates the position and underestimates the height of this peak. The inclusion of the polarization represents a certain improvement in the description of this peak, although it still appears at somewhat larger r values than in the experimental function. The fact that the shorter is the distance where this hydrogen-bonding peak appears, the higher the peak is, reflects that the hydrogen-bonding coordination number is the same (i.e., about 2) for all the three models. It is also clear that, in spite of the fact that the hydrogen-bonding peak of the JV-NP model appears at 0.15 Å shorter distance than the experimental one, this model reproduces very well the low r side of this peak, including the soft-core diameter of the hydrogen-bonding interaction of 1.15 Å. Surprisingly, the other two models result in a soft-core diameter of 1.45 Å, in spite of the fact that the position of the peak is much better reproduced by the polarizable model than either by JV-NP or by TIPS. Although the obtained closest H$\cdots$F approach is obviously related to the Lennard-Jones σ parameter of the model (the TIPS and JV-P models both have a 0.2 Å larger σ value than JV-NP; see Table I) this relation is rather complex. First, because the Lennard-Jones interaction is only acting between F atoms in these models, and second, because, due to the Coulombic interactions, the F$\cdots$F separation of two molecules corresponding to their minimum energy arrangement is considerably shorter than the value of σ, and hence the Lennard-Jones contribution to their pair interaction energy is strongly repulsive.[30–32] However, the present results suggest that, in spite of this complexity, hydrogen-bonding soft-core diameter strongly correlates to the value of the σ parameter of the model.

The experimental $G(r)$ function shows a clear second peak at 2.55 Å, followed by a low and broad, slightly splitted third peak. The second peak, reflecting the H–H and F–F correlations of the hydrogen-bonded neighbors,[31,32] is somewhat overemphasized for the JV-NP model. The polarizable model reproduces the correct height of this peak; however, it appears at about a 0.15 Å higher value. This peak is almost completely missing on the $G(r)$ function of the TIPS model (only a small shoulder at about 2.85 Å might be assigned to this peak). The H$\cdots$H and F$\cdots$F distances of the hydrogen-bonding pairs are determined by the hydrogen-bonding H$\cdots$F distance and the H–F$\cdots$H and F$\cdots$H–F angles. Therefore, the absence of this second peak of $G(r)$ indicates that the TIPS model does not reproduce well the relative arrangement of the hydrogen-bonding pairs around each other. The broad third peak, as well as the following minimum of the experimental $G(r)$, is reasonably well reproduced by the two nonpolarizable models. On the other hand, the polarizable model results in a higher peak and deeper minimum, indicating that this model overestimates the relative ordering of the more distant neighbors in the hydrogen-bonding chains.

Comparisons at the higher temperature state points lead to conclusions similar to those at state point I. The closest approach of the neighboring molecules is well reproduced by the JV-NP model at every state point, whereas the other two models always overestimate it by 0.3 Å. The first peak of the JV-NP model always appears at shorter distances and is always higher than the corresponding experimental one. Moreover, at state points IV–VI the second peak of this model also appears to be at too low r values and it is too high. On the other hand, the TIPS and JV-P models show smaller peaks at larger r values than the corresponding experimental

functions. It is also apparent that at the high temperature state points the $G(r)$'s obtained with these two models become rather similar to each other. When the temperature or the density of the system is increased, the first peak of the experimental $G(r)$ function becomes lower, and the following minimum higher. This trend is present in the $G(r)$'s of all three models; moreover, it is clearly exaggerated by TIPS, which gives only a shoulder instead of this peak at state points III and IV. The second and third peak of the experimental $G(r)$ becomes less separated at the high temperature liquid state point II than at state point I, and they merge to a single splitted peak above the critical point. The simulated $G(r)$'s of the JV-NP and JV-P models undergo similar changes with increasing temperature and decreasing density, and reproduce these features at least qualitatively. Since the separate second peak of the experimental $G(r)$ disappears at 473 K, even the results of the TIPS model are in a qualitative agreement with the experimental data at this temperature.

In spite of the general ability of the three models to reproduce, at least qualitatively, the changes in the main features of the experimental pair correlation functions, there is an important difference among them concerning the description of the elongation of the hydrogen bonds with increasing temperature and decreasing density. In order to analyze this effect, we have fitted a Gaussian function to the rising side of the first peak of the $G(r)$'s, up to the maximum. We have excluded the descending side of the peak from the fitting because correlations other than those concerning the hydrogen-bonding H–F pairs can also contribute to the $G(r)$ in this region. We have estimated the average hydrogen bond length in a system by the position of the maximum of this fitted Gaussian function. This analysis shows that the hydrogen bonds are elongated by 0.18 Å in real HF when moving from state point I to state point VI. This effect is underestimated by all the three models, as the shift of the center position of the fitted Gaussian functions is only 0.11 Å, 0.08 Å, and 0.10 Å for the JV-P, JV-NP, and TIPS model, respectively. The difference between the behavior of the polarizable and nonpolarizable models in this respect becomes apparent when the change of the hydrogen bond length is solely due to the decrease of the density. Figure 3 shows the position of the center of the fitted Gaussians as a function of the density along the $T=473$ K isotherm. For better comparison, the results are shifted by r^{III}, i.e., the value obtained at state point III. It is clear that only the polarizable JV-P model reproduces the experimentally observed shortening of the hydrogen bonds with increasing density, even if this shortening is not large enough for the model. On the other hand, the average hydrogen bond length is found to be independent from the density of the system for the nonpolarizable models. This finding is consistent with our previous result that only the polarizable model can reproduce the elongation of the F$\cdots$F separation of a hydrogen-bonded HF pair when moving from ambient liquid to the isolated dimer.[32] The present result is also in agreement with the recent finding that also for water only polarizable models can reproduce the experimentally observed elongation of the average hydrogen bond length when the system is moved from ambient to supercritical conditions.[10,11]

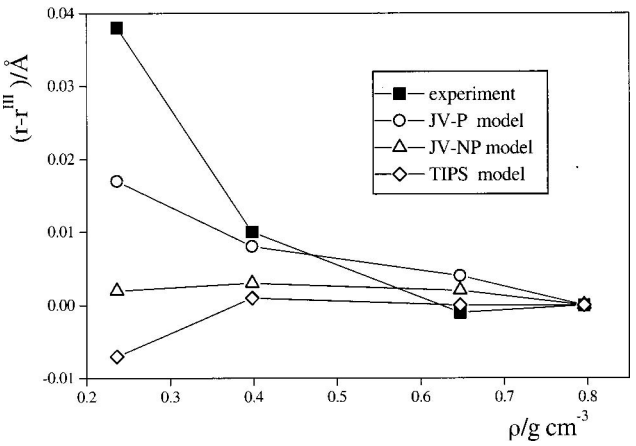

FIG. 3. Position of the center of the Gaussian function fitted to the rising side of the first peak of the $G(r)$ total pair correlation function of deuterated HF as a function of the density at $T=473$ K. For better visualization, the results are shifted by r^{III}, the center of the Gaussian obtained at state point III.

V. THERMODYNAMIC RESULTS

The most important thermodynamic properties of the three models are summarized and compared with experimental data at all the six state points in Table III. The simulated density values are obtained from simulations performed on the (N,p,T) ensemble. As is evident, at state point I the experimental density is reproduced well (i.e., within 4% and 1%, respectively) by the JV-P and the TIPS model, whereas it is seriously overestimated by the JV-NP model. The latter finding is rather surprising, since this model has proved to be able to reproduce the experimental density very accurately at the nearby thermodynamic state point of $\{T=273\,\mathrm{K},\ p=1\,\mathrm{bar}\}$.[31] The reason for this sudden failure of the JV-NP model in reproducing the experimental density at state point I can be understood by considering that the density of this model depends only very weakly on the corresponding equilibrium energy.[31] As a consequence, a small variation of the thermodynamic conditions, which results only in a small change of the energy, might lead to unusually large changes in the density of the system. This weak dependence of the density on the energy of the JV-NP system also leads to the unusually large fluctuations of its local density, which has been reported recently.[13]

At the high temperature liquid state point II the JV-NP model is found to be in the vapor phase. However, since this state point is along the experimental liquid–vapor coexistence curve, this finding does not necessarily indicate a serious failure of the model. The density of the polarizable JV-P model agrees again very well, within 3%, with the experimental value. Considering also the fact that this model reproduces the density of liquid HF within the same error even at the state point $\{T=203\,\mathrm{K},\ p=1\,\mathrm{bar}\}$, i.e., close to the freezing point of HF, we can conclude that the JV-P model can well describe the density of HF in the entire range of existence of its liquid state, covering an almost 200 K wide temperature interval. It is also apparent that the density of the model is always about 3%–4% lower than the experimental value, indicating that (i) there might have been some small

TABLE III. Thermodynamic properties of the tested HF models at six thermodynamic state points. Results are obtained from simulations on the (N,V,T) ensemble, unless otherwise indicated. Experimental data are shown for comparisons.

State point	Model	ρ/g cm^{-3} [a]	U/kJ mol^{-1}	c_V/J mol^{-1} K^{-1}	μ/D
	JV-P	0.924±0.028	−26.42±0.34	61.5	2.17±0.49
I	JV-NP	1.230±0.032	−27.28±0.32	56.7	1.83
$T=300$ K	TIPS	0.971±0.058	−24.84±0.29	50.0	2.04
	Experiment	**0.962**[b]	**−27.74**[c] **(−28.22)**[d]	**47.6**[e]	
	JV-P	0.774±0.039	−22.47±0.43	62.6	2.11±0.42
II	JV-NP	0.0188±0.0003	−23.80±0.43	60.9	1.83
$T=373$ K	TIPS	0.633±0.041	−21.87±0.35	47.3	2.04
	Experiment	**0.796**[b]	**−25.51**[c,f] **(−23.08)**[d]	**56.7**[e,f]	
	JV-P	0.584±0.050	−19.41±0.40	43.0	2.07±0.34
III	JV-NP	0.615±0.077	−20.37±0.46	49.5	1.83
$T=473$ K	TIPS	0.579±0.039	−19.60±0.38	40.6	2.04
	Experiment	**0.796**[b]	**(−27.49)**[d]	**55.0**[e,g]	
	JV-P	0.334±0.047	−17.92±0.42	45.6	2.06±0.32
IV	JV-NP	0.294±0.024	−19.45±0.48	52.3	1.83
$T=473$ K	TIPS	0.423±0.041	−18.18±0.41	43.9	2.04
	Experiment	**0.647**[b]	**(−23.39)**[d]	**59.5**[e,g]	
	JV-P	0.081±0.07	−15.09±0.48	52.8	2.04±0.24
V	JV-NP	0.097±0.011	−17.42±0.52	57.7	1.83
$T=473$ K	TIPS	0.091±0.016	−15.63±0.45	49.2	2.04
	Experiment	**0.398**[b]	**(−19.83)**[d]	**76.1**[e,g]	
	JV-P	0.068±0.005	−12.08±0.59	68.0	2.02±0.08
VI	JV-NP	0.073±0.008	−15.66±0.58	66.7	1.83
$T=473$ K	TIPS	0.081±.007	−13.62±0.49	53.2	2.04
	Experiment	**0.236**[b]	**(−19.75)**[d]	**112.6**[e,g]	

[a]Results obtained from (N,p,T) ensemble simulations.
[b]Reference 49.
[c]Data taken from Ref. 60, using the relation $U=-\Delta H^{\circ}_{\text{vap}}+RT$, where $\Delta H^{\circ}_{\text{vap}}$ is the heat of vaporization to ideal gas.
[d]Values in parenthesis are resulted from the Visco–Kofke equation-of-state (Ref. 61).
[e]Reference 62.
[f]Value obtained from published experimental data by linear extrapolation.
[g]Value obtained from published experimental $c_V(\rho)$ data along the $T=473$ K isotherm by interpolation.

inaccuracies in the parameterization of the model, which have led to this constant density shift, and (ii) the *change* of the density of liquid HF due to the variation of the thermodynamic conditions is accurately described by the JV-P model. It is also evident from Table III that at state point II the TIPS model underestimates the experimental density value by about 20%, whereas at the low temperature state point $\{T=203\,\text{K},\ p=1\,\text{bar}\}$ its density is about 10% *higher* than the experimental value.[31] This means that, similarly to the JV-NP model, the density of the TIPS model also changes in a different way with the thermodynamic conditions than that of real HF. Both of these nonpolarizable models reproduce the experimental density value at the state point of $\{T=273\,\text{K},\ p=1\,\text{bar}\}$, at which they have been parameterized,[30,31] whereas they may lead to wrong densities at different thermodynamic states. These findings lead us to conclude that the ability of the JV-P model to well describe the temperature and pressure dependence of the density of HF in the entire range of existence of its liquid state can be attributed to the explicit description of the polarization of the molecules, and thus to the accurate modeling of their average dipole moment in the liquid under all kinds of thermodynamic conditions. This result is in clear contrast with the recent findings for water, where the density of various different polarizable models has been found to decrease too rapidly with increasing temperature.[4,8–11,14,15]

At the four supercritical state points all three models strongly underestimate the experimental density values, indicating that above the critical point even the polarizable JV-P model cannot describe well the density of the system. It is also seen that the density of the three models still depends on the pressure in a different way (e.g., at state point III the JV-NP model results in the largest, whereas at state point IV the smallest density value among the three models). These deviations are originated by the fact that the critical point of the models differs from that of real HF, and therefore a given supercritical state point represents rather different thermodynamic conditions for the different models and for real HF in terms of reduced thermodynamic parameters (i.e., $T/T^c, p/p^c, \rho/\rho^c$, where T^c, p^c, and ρ^c are the critical temperature, pressure, and density, respectively).

Due to these large deviations of the simulated densities from the experimental values at the supercritical state points, and to the fact that at the liquid state point II the JV-NP model is in the vapor phase, we have decided to compare the other thermodynamic quantities on the basis of the (N,V,T) ensemble simulations, as also done in the analysis of the pair correlation functions. Since we could not find any experi-

mental information on the internal energy of supercritical HF, we have regarded results of the Visco–Kofke equation-of-state[61] as ''experimental data'' here.

As is evident, at state point I both the JV-NP and the JV-P models reproduce well (within about 2% and 5%, respectively) the experimental configurational energy of the system. On the other hand, the energy of the TIPS model is about 10% higher than the experimental value. This is due to the fact that in the parameterization of this model no long range correction was taken into account for the electrostatic interactions.[30] At state point II the JV-NP model again gives the lowest and the TIPS the highest energy value. Now the energy of all the three models is considerably, by 7%–15%, higher than the experimental value. However, it should be noted that there is no experimental energy value available above 329 K, the value of -25.51 kJ/mol given here is obtained by a linear extrapolation from the experimental energy data measured between 293 K and 329 K.[60] Considering the value resulted from the Visco–Kofke equation-of-state[61] instead, an agreement within 3% is found with the results of both the JV-P and JV-NP models, whereas the TIPS model gives an about 5% higher energy value.

The energy of the system is rather low at the supercritical states, as seen from the Visco–Kofke equation-of-state. This indicates that the HF molecules can form strong hydrogen bonds with each other, building up small hydrogen-bonded clusters even above the critical point. Still, it is rather striking that the energy of the dense supercritical state III is considerably lower than that of the liquid state point II, which corresponds to the same density. Despite their rather low energies at the supercritical state points, all three models show considerably less and weaker association than the Visco–Kofke equation-of-state. Thus at state point III all the models result in higher energy values than at state point II, and at the lowest density state point VI their energy is about 50% of that at state point I, in contrast to the results of the Visco–Kofke equation-of-state, for which this ratio is about 70%.

It is also apparent that, similarly to the $G(r)$ functions, the configurational energy of the JV-P and TIPS models also becomes rather similar to each other at the supercritical state points. The similarity of the two models at these thermodynamic states can be explained by the fact that, due to the decrease of the density, the average dipole moment of the molecules in the polarizable JV-P model is smaller here than at the liquid state points, becoming roughly equal to the fixed molecular dipole moment value of 2.04 D of the nonpolarizable TIPS model.

The constant volume heat capacity c_V of a system can be calculated in a simulation as

$$c_V = \frac{\langle U^2 \rangle - \langle U \rangle^2}{k_B T} + \frac{5}{2} R, \tag{10}$$

where the first term stands for the configurational, and the second for the kinetic part of the heat capacity. In this equation k_B is the Boltzmann constant, R is the gas constant, and $\langle ... \rangle$ denotes ensemble averaging. Since c_V is related to the fluctuation of the energy of the system, it can only be determined with a considerably larger inaccuracy in a simulation than the energy itself. As shown in Table III, at state point I the heat capacity of the TIPS model agrees quite well with the experimental value, whereas the JV-NP and JV-P models overestimate it by 20%–30%. At state point II the situation is the opposite; here the c_V value of both the JV-P and JV-NP models is in considerably better agreement with the experimental data than that of TIPS, which underestimates it by about 15%. At the four supercritical state points all three models result in heat capacities that are considerably, by about 10%–50% lower than the experimental values.

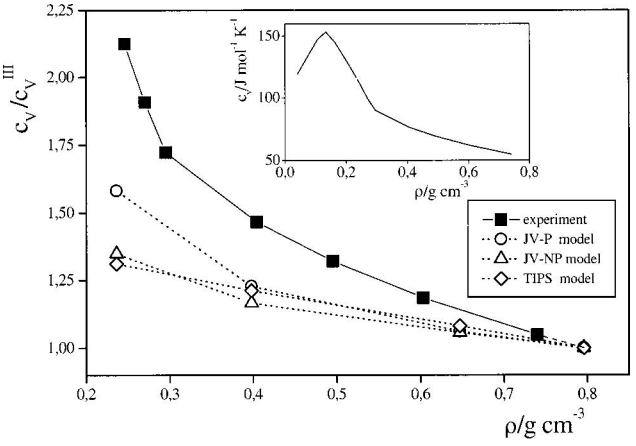

FIG. 4. Constant volume heat capacity c_V of hydrogen fluoride as a function of the density along the supercritical isotherm of $T=473$ K. Experimental data are taken from Ref. 62. For better comparison, heat capacities are shown in reduced units, i.e., normalized by c_V^{III}, the value corresponding to the density of state point III of 0.796 Å^{-3}. The inset shows the experimental $c_V(\rho)$ function in a wider density range.

It is interesting to compare the density dependence of the heat capacity c_V of the three models with that of real HF along the supercritical isotherm of $T=473$ K. Fortunately, experimental data have been reported at several densities at this temperature.[62] The comparison in the density range covering state points III–VI is shown in Fig. 4. For completeness, the experimental $c_V(\rho)$ curve is shown in the inset of the figure in the entire density range in which it has been measured. Since we compare here the *dependence* of c_V on the density of the system rather than the actual c_V values themselves, Fig. 4 shows the compared heat capacities in reduced units, i.e., c_V/c_V^{III} is plotted instead of c_V, where c_V^{III} is the value corresponding to 0.796 g/cm^3, i.e., the density of state point III. As is seen in the inset, the experimental $c_V(\rho)$ curve goes through a rather sharp maximum at about 0.13 g/cm^3. The presence of this maximum is the consequence of the vicinity of the critical point. In the p-T plane, the line connecting the points at which the various supercritical $c_V(\rho)$ isotherms have a maximum originates from the critical point, and represents the supercritical extension of the vapor–liquid coexistence curve, along which c_V is infinite. As seen in Fig. 4, the range of the simulated densities is on the descending side of this peak for all three models. It is also seen that the steepness of all three simulated functions is considerably smaller than that of the experimental curve. Among the three simulated functions the one obtained with the JV-P model is clearly in better agreement with the experimental line than that of the two nonpolarizable models. The

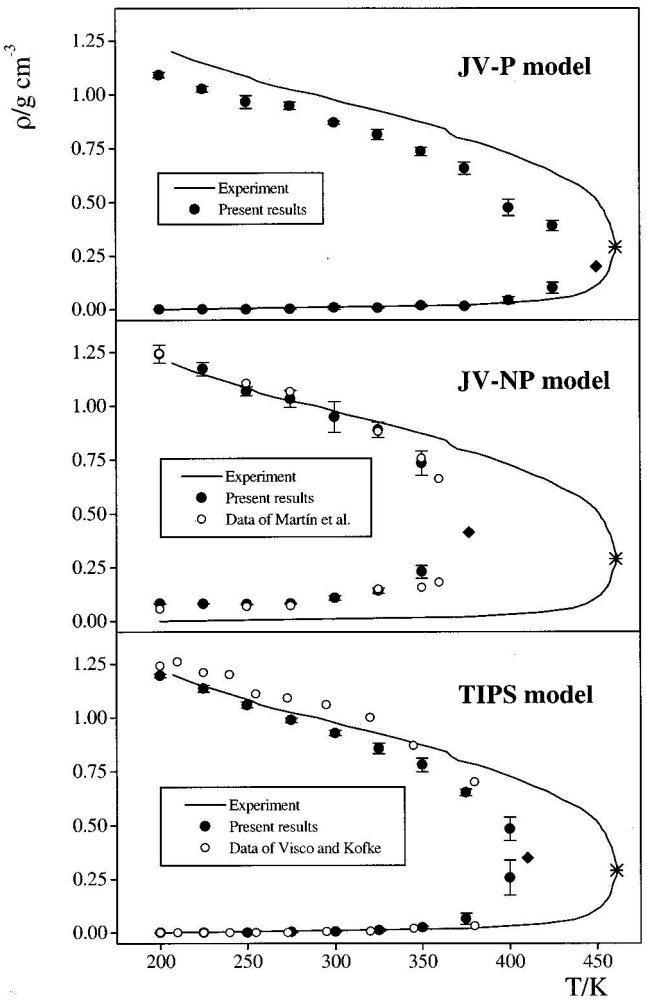

FIG. 5. Comparison of the vapor–liquid coexistence curve of (a) the JV-P, (b) the JV-NP, and (c) the TIPS model with experimental data (Refs. 45, 62). Error bars are only shown when larger than the symbols themselves. Results of the Gibbs ensemble Monte Carlo simulations of Martín *et al.* with the JV-NP model (Ref. 47) and those of the Gibbs–Duhem integration of Visco and Kofke with the TIPS model (Refs. 45, 46) are also shown. The estimated critical point of the models is shown as ◆; the experimental critical point is indicated by *.

smaller steepness of the simulated functions suggests that the corresponding heat capacity maximum might also be smaller for these models than for real HF. Since this peak of $c_V(\rho)$ is infinitely high at the critical temperature, and its height should decrease when moving toward higher temperature isotherms, the present result suggests that (i) the critical point of all the three models is below the critical temperature of real HF, and (ii) the critical temperature of the polarizable JV-P model, which have the steepest $c_V(\rho)$ isotherm at 473 K, is much closer to the experimental value than that of the two nonpolarizable models. This point is further investigated in the following section.

VI. VAPOR–LIQUID EQUILIBRIUM

The vapor–liquid coexistence curve of the three models, obtained from GEMC simulations, is shown and compared with experimental data[45,62] in Fig. 5. For comparison, results of a previous GEMC study of Martín *et al.* with the JV-NP model[47] and of a Gibbs–Duhem integration study of Visco and Kofke with the TIPS model[45,46] are also shown. The phase envelope obtained for the JV-NP model is in a good agreement with the results of Martín *et al.*,[47] whereas the density of the coexisting liquid phase obtained with the TIPS model is systematically smaller than the results of Visco and Kofke.[45,46] The reason for this discrepancy is that Visco and Kofke have not used any long-range correction for the electrostatic interactions, whereas in the present study reaction field correction has been applied.

TABLE IV. Critical constants of the three models investigated, as obtained by fitting a fourth order polynomial to the simulated $T(\rho)$ data at the four highest temperatures at which phase separation has been observed. Values in parenthesis are obtained by fitting a third order polynomial to the $\Delta\rho(T)$ and a straight line to the $\overline{\rho}(T)$ function.

	JV-P	JV-NP	TIPS	Experiment[a]
T^c/K	450 (453)	377 (387)	410 (413)	461
ρ^c/g cm^{-3}	0.200 (0.198)	0.414 (0.435)	0.350 (0.334)	0.290

[a]Reference 62.

In order to determine the critical parameters of the models we have fitted a fourth order polynomial to the simulated $T(\rho)$ data at the four highest temperatures at which phase separation has been observed. The position and the value of the maximum of this fitted function have then been taken as the critical density ρ^c and critical temperature T^c, respectively. The resulting critical parameters are summarized and compared with the experimental values in Table IV. In order to check the validity of this method we have estimated T^c and ρ^c in a different way, as well. Thus we have fitted a third order polynomial to the obtained points of the $\Delta\rho(T)$ function, where $\Delta\rho=\rho_{\mathrm{liq}}-\rho_{\mathrm{vap}}$. (Indices "liq" and "vap" refer to the liquid and vapor phase, respectively.) The critical temperature is estimated as the value at which this fitted function reaches zero. In getting the value of the critical density ρ^c a linear function has been fitted to the simulated $\overline{\rho}(T)$ points, where $\overline{\rho}=(\rho_{\mathrm{liq}}-\rho_{\mathrm{vap}})/2$, and the density value corresponding to T^c along this fitted line has been determined. The critical parameters obtained in these two different ways have always been found in a good agreement (i.e., within 10 K for T^c and within 0.02 g/cm^{-3} for ρ^c) with each other. The T^c and ρ^c values obtained in the latter way are also included in Table IV.

As is seen from Fig. 5 and Table IV, the results obtained confirm our previous conclusions. Indeed, the critical point of all the three models is below the experimental critical temperature, and also the T^c value of the polarizable JV-P model is much closer to the experimental value than that of the other two models. It is also seen in the top part of Fig. 5 that in the liquid side of the coexistence curve the JV-P model follows well the shape of the experimental function, however, consistently with our previous findings, it is shifted toward smaller densities. On the other hand, the two nonpolarizable models can reproduce well the density of the coexisting liquid phase at low temperatures, whereas above 300 K the simulated liquid densities decrease rapidly with increasing temperature, leading to too low T^c values. It is also seen that the vapor density values of the JV-NP model are

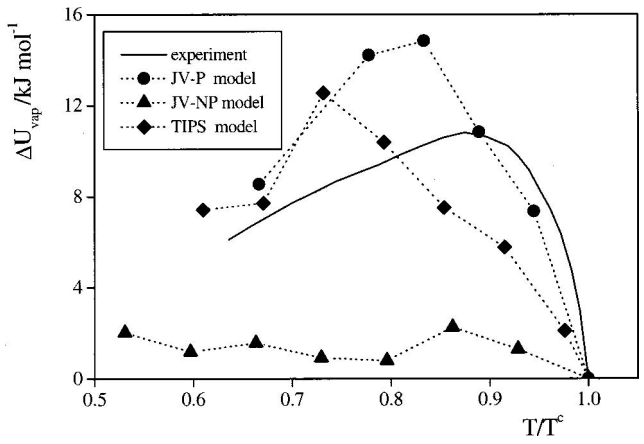

FIG. 6. Comparison of the energy of vaporization of the three HF models studied as a function of the reduced temperature T/T^c with experimental data (Ref. 62).

shifted toward higher densities with respect to the experimental curve, indicating that in this model the hydrogen-bonded clusters in the gas phase are too large.

The heat and energy of vaporization (ΔH_{vap} and ΔU_{vap}, respectively) of hydrogen fluoride has an unusual temperature dependence, as both $\Delta H_{vap}(T)$ and $\Delta U_{vap}(T)$ go through a maximum at around 400 K.[62] This unusual behavior indicates that the HF molecules form small but strongly hydrogen-bonded clusters in the vapor phase even at low temperatures. It has been shown by Visco and Kofke[45,46] that potential models based on *ab initio* calculations of small HF clusters cannot reproduce this behavior, they result in a monotonously decreasing $\Delta H_{vap}(T)$ function instead. We have calculated the energy of vaporization of the three models investigated from the results of the GEMC simulations, as $\Delta U_{vap}=U_{vap}-U_{liq}$. The results are shown and compared with the experimental curve as a function of the reduced temperature T/T^c in Fig. 6. Contrary to the *ab initio* based potentials, all three models tested here can reproduce the main feature of the experimental curve, at least in a qualitative way, as their $\Delta U_{vap}(T)$ functions all go through a maximum. This maximum is located at somewhat lower reduced temperatures in the simulated functions (i.e., at about 0.83 for the JV-P and JV-NP, and at 0.73 for the TIPS model) than the experimental maximum position of 0.87. However, besides the qualitative reproduction of the presence of this maximum, the three simulated $\Delta U_{vap}(T)$ curves show strong differences. The TIPS and JV-P models reproduce the experimental curve reasonably well, although the maximum is clearly too high for both of these models. On the other hand, the JV-NP model gives very low ΔU_{vap} values. This latter finding is consistent with our previous result that the density of the coexisting vapor phase of this model is considerably larger than the experimental data. Both of these features originate from the fact that the JV-NP model results in too strong an attraction between the molecules in the gas phase, which leads to too large clusters with too low energy. This observation is also consistent with our previous finding that very large density variations of this model are associated with unusually small changes in the energy of the system,[31] and hence the model shows large fluctuations in the local density.[13] The present results suggest that this feature of the JV-NP model might not correspond to a real physical behavior. However, such a conclusion should be confirmed by determining the local density fluctuations in liquid HF by small angle neutron or x-ray scattering experiment.

VII. CONCLUSIONS

In this study the structural and thermodynamic properties of a polarizable and two pairwise additive effective potential models of hydrogen fluoride have been compared at several liquid and supercritical state points as well as in vapor–liquid equilibrium. Previous studies have shown that, due to the great importance of the cooperative effects, effective models can, in general, reproduce the properties of HF in the liquid phase much better than models parameterized on the basis of *ab initio* calculations of HF dimers and oligomers. The present study has shown that, in addition to this observation, some of the vapor–liquid equilibrium properties of HF are also better described by effective than by *ab initio* based potentials. In particular, contrary to the failure of several models of the latter type,[45,46] all three effective models investigated here reproduce the experimental fact[62] that the energy of evaporation of HF does not decrease monotonously with increasing temperature, but goes through a maximum instead. This unusual behavior of the energy of evaporation of HF clearly shows that there is only a rather weak correlation between its density and internal energy (i.e., the energy of the coexisting low density vapor and high density liquid phases are rather close to each other, even at low temperatures). Therefore, the success of the effective potential models, especially of TIPS and JV-P, in reproducing the main features of the $\Delta U_{vap}(T)$ function is of great importance, since it also implies the reproduction of this weak correlation between the density and the energy of the system. On the other hand, some results of the present study suggest that the strength of this weak correlation is even underestimated by the JV-NP model. Thus the liquid density of the model is found to change much too rapidly with the thermodynamic conditions, at least in some regions of the phase diagram. Moreover, the density of the coexisting vapor phase is overestimated along the entire vapor–liquid coexistence curve, and consistently, the energy of evaporation is underestimated by the model. These findings are also consistent with the recent result that the JV-NP model leads to rather large fluctuations of the local density of the system.[13] Clarification of the real behavior of hydrogen fluoride in this respect needs further investigation, including studies of small angle scattering experiments in the liquid phase.

Comparison of the three models have revealed that the explicit inclusion of the polarization in the model indeed leads to a significant improvement of its performance, as the polarizable JV-P model has proved to be superior over the two pairwise additive models in various respects. First, it reproduces the structure of liquid HF better than the two nonpolarizable models. More importantly, the *change* of the structure due to the variation of the thermodynamic conditions (i.e., the elongation of the hydrogen bonds with decreasing density) is much better described by the polarizable model than by the pairwise additive ones. This finding is in agreement with the results of a similar comparison between

polarizable and nonpolarizable water models.[10,11] Similarly, among the three models only JV-P describes well the dependence of the liquid density on the temperature and pressure in the entire range of existence of the liquid state. As a consequence, this model also reproduces well the steepness of the liquid side of the vapor–liquid coexistence curve, which leads also to a much better reproduction of the critical temperature of HF than that of the nonpolarizable models. Moreover, the better reproduction of the critical point leads to a better agreement in the reduced thermodynamic parameters in the supercritical state, and hence to a better reproduction of the properties of supercritical HF, as demonstrated by the density dependence of the heat capacity at 473 K. This success of the polarizable model in describing the properties of HF in a broad range of thermodynamic states, including states of vapor–liquid equilibrium, can be explained by the fact that this model can, at least partly, account for the large cooperativity of the molecules. Thus the polarizable model can take explicitly into account the change of the molecular dipole moment with the thermodynamic conditions, especially with the density. On the other hand, nonpolarizable models have been parameterized in order to account for the polarization of the molecules at one specific state point (usually at ambient conditions) only. Hence, these models fail to reproduce the local electric environment of the molecules at thermodynamic state points being far from where the model has been parameterized.

The results of the present study also suggest that many of the discrepancies observed between the properties of the JV-P model and of real HF are originated from the fact that, due to some inaccuracies in the parameterization, the model results in a somewhat too low liquid density. On the other hand, the dependence of the density on the thermodynamic conditions is well described by the model; this density shift persists in the entire liquid range, including also the liquid states of the vapor–liquid equilibrium. Therefore, this density shift can also be responsible for the shift of the critical point of the model, and thus for at least some of its discrepancies in the supercritical phase. A careful reparameterization of the model might eliminate most of these discrepancies, and considerably improve its performance in a wide range of thermodynamic states. Considering also the fact that, contrary to the JV-NP model, JV-P overestimates the soft-core diameter of the H$\cdots\cdots$F interaction, and also taking into account the strong correlation observed between this diameter and the σ Lennard-Jones parameter, it seems to be rather likely that in such a reparameterization the value of σ should be decreased, and its new value should be close to that of the JV-NP model. Work in this direction is in progress.

ACKNOWLEDGMENT

The authors are grateful to Dr. Till Pfleiderer (University of Stuttgart, Germany) for kindly providing the experimental pair correlation functions, and to Dr. Donald P. Visco (Tennessee Technological University) for providing the internal energy values as calculated by the Visco–Kofke equation-of-state. We are also grateful to Dr. Pfleiderer and Dr. Visco to provide several references to various experimental thermodynamic quantities of HF.

[1] P. H. Poole, F. Sciortino, U. Essmann, and H. E. Stanley, Nature (London) **360**, 324 (1992).
[2] J. P. Brodholt, M. Sampoli, and R. Vallauri, Mol. Phys. **86**, 149 (1995).
[3] A. A. Chialvo and P. T. Cummings, J. Chem. Phys. **105**, 8274 (1996).
[4] I. M. Svishchev, P. G. Kusalik, J. Wang, and R. J. Boyd, J. Chem. Phys. **105**, 4742 (1996).
[5] A. G. Kalinichev and J. D. Bass, J. Phys. Chem. A **101**, 9720 (1997).
[6] F. Sciortino, P. H. Poole, U. Essmann, and H. E. Stanley, Phys. Rev. E **55**, 727 (1997).
[7] P. Jedlovszky, J. P. Brodholt, F. Bruni, M. A. Ricci, A. K. Soper, and R. Vallauri, J. Chem. Phys. **108**, 8528 (1998).
[8] K. Kiyohara, K. E. Gubbins, and A. Z. Panagiotopoulos, Mol. Phys. **94**, 803 (1998).
[9] P. Jedlovszky and R. Vallauri, Mol. Phys. **97**, 1157 (1999).
[10] P. Jedlovszky and J. Richardi, J. Chem. Phys. **110**, 8019 (1999).
[11] P. Jedlovszky, R. Vallauri, and J. Richardi, J. Phys.: Condens. Matter **12**, A115 (2000).
[12] P. Jedlovszky, M. Mezei, and R. Vallauri, Chem. Phys. Lett. **318**, 155 (2000).
[13] P. Jedlovszky, J. Chem. Phys. **113**, 9113 (2000).
[14] J. Kolafa and I. Nezbeda, Mol. Phys. **98**, 1505 (2000).
[15] P. Jedlovszky and R. Vallauri, J. Chem. Phys. **115**, 3750 (2001).
[16] M. E. van Leeuwen and B. Smit, J. Phys. Chem. **99**, 1831 (1995).
[17] N. Asahi and Y. Nakamura, J. Chem. Phys. **109**, 9879 (1998).
[18] I. Y. Shilov, B. M. Rode, and V. A. Durov, Chem. Phys. **241**, 75 (1999).
[19] I. Bakó, P. Jedlovszky, and G. Pálinkás, J. Mol. Liq. **87**, 243 (2000).
[20] M. A. González, E. Enciso, F. J. Bermejo, and M. Bée, J. Chem. Phys. **110**, 8045 (1999).
[21] C. Benmore and Y. L. Loh, J. Chem. Phys. **112**, 5877 (2000).
[22] P. Jedlovszky, I. Bakó, G. Pálinkás, and J. C. Dore, Mol. Phys. **86**, 87 (1995).
[23] P. Jedlovszky and L. Turi, J. Phys. Chem. A **101**, 2662 (1997); *ibid.* erratum **103**, 3796 (1999).
[24] P. Jedlovszky and L. Turi, J. Phys. Chem. B **101**, 5429 (1997); *ibid.* erratum **103**, 3510 (1999).
[25] P. Mináry, P. Jedlovszky, M. Mezei, and L. Turi, J. Phys. Chem. B **104**, 8287 (2000).
[26] T. Kristóf, J. Vorholz, J. Liszi, B. Rumpf, and G. Maurer, Mol. Phys. **97**, 1129 (1999).
[27] M. Diraison, G. J. Martyna, and M. E. Tuckerman, J. Chem. Phys. **111**, 1096 (1999).
[28] M. Deraman, J. C. Dore, J. G. Powles, J. H. Holloway, and P. Chieux, Mol. Phys. **55**, 1351 (1985).
[29] M. L. Klein and I. R. McDonald, J. Chem. Phys. **71**, 298 (1979).
[30] M. E. Cournoyer and W. L. Jorgensen, Mol. Phys. **51**, 119 (1984).
[31] P. Jedlovszky and R. Vallauri, Mol. Phys. **92**, 331 (1997).
[32] P. Jedlovszky and R. Vallauri, J. Chem. Phys. **107**, 10166 (1997).
[33] R. G. Della Valle and D. Gazzillo, Phys. Rev. B **59**, 13699 (1999).
[34] M. L. Klein, I. R. McDonald, and S. F. O'Shea, J. Chem. Phys. **69**, 63 (1978).
[35] W. L. Jorgensen and M. E. Cournoyer, J. Am. Chem. Soc. **100**, 4942 (1978).
[36] W. L. Jorgensen, J. Chem. Phys. **70**, 5888 (1979).
[37] U. Röthlisberger and M. Parrinello, J. Chem. Phys. **106**, 4658 (1997).
[38] P. Jedlovszky and R. Vallauri, Mol. Phys. **93**, 15 (1998).
[39] R. L. Redington, J. Chem. Phys. **75**, 4417 (1981).
[40] C. Zhang, D. L. Freeman, and J. D. Doll, J. Chem. Phys. **91**, 2489 (1989).
[41] U. Balucani, G. Garberoglio, G. Sutmann, and R. Vallauri, Chem. Phys. Lett. **315**, 109 (1999).
[42] U. Balucani, D. Bertolini, G. Sutmann, A. Tani, and R. Vallauri, J. Chem. Phys. **111**, 4663 (1999).
[43] D. Bertolini, G. Sutmann, A. Tani, and R. Vallauri, Phys. Rev. Lett. **81**, 2080 (1998).
[44] G. Garberoglio and R. Vallauri, Phys. Rev. Lett. **84**, 4878 (2000).
[45] D. P. Visco, Jr. and D. A. Kofke, J. Chem. Phys. **109**, 4015 (1998).
[46] D. P. Visco, Jr. and D. A. Kofke, Fluid Phase Equilib. **158–160**, 37 (1999).
[47] C. Martín, M. Lombardero, J. A. Anta, and E. Lomba, J. Chem. Phys. **114**, 355 (2001).
[48] P. H. Fries and J. Richardi, J. Chem. Phys. **113**, 9169 (2000).
[49] T. Pfleiderer, I. Waldner, H. Bertagnolli, K. Tödheide, and H. E. Fischer, J. Chem. Phys. **113**, 3690 (2000).
[50] J. A. Barker and R. O. Watts, Mol. Phys. **26**, 789 (1973).
[51] M. Neumann, J. Chem. Phys. **82**, 5663 (1985).
[52] G. Ruocco and M. Sampoli, Mol. Phys. **82**, 875 (1994).

[53] M. P. Allen and D. J. Tildesley, *Computer Simulation of Liquids* (Oxford University Press, Oxford, 1987).
[54] A. Z. Panagiotopoulos, Mol. Phys. **61**, 813 (1987).
[55] M. Mezei, Mol. Simul. **9**, 257 (1992).
[56] M. Mezei, Mol. Phys. **40**, 901 (1980).
[57] M. Mezei, Mol. Phys. **61**, 565 (1987); *ibid.* erratum **67**, 1207 (1989).
[58] P. Ahlström, A. Wallquist, S. Engström, and B. Jönsson, Mol. Phys. **68**, 563 (1989).
[59] M. Alfredsson, J. P. Brodholt, K. Hermansson, and R. Vallauri, Mol. Phys. **94**, 873 (1998).
[60] C. E. Vanderzee and W. W. Rodenburg, J. Chem. Thermodyn. **2**, 461 (1970).
[61] D. P. Visco and D. A. Kofke, Ind. Eng. Chem. Res. **38**, 4125 (1999); *ibid.* erratum **39**, 242 (2000).
[62] E. U. Franck and W. Spalthoff, Z. Elektrochem. **61**, 348 (1957).